Plant Physiology and Biochemistry 196 (2023) 130–138

Contents lists available at ScienceDirect

Plant Physiology and Biochemistry

journal homepage: www.elsevier.com/locate/plaphy

Synthesis of phytostabilized zinc oxide nanoparticles and their effects on physiological and anti-oxidative responses of *Zea mays* (L.) under chromium stress

Musarrat Ramzan [a], Gul Naz [b], Anis Ali shah [c], Misbah Parveen [a], Muhammad Jamil [a], Sidra Gill [a], Hafiz M.Adeel Sharif [d,*]

[a] Department of Botany, Faculty of Chemical and Biological Sciences, The Islamia University of Bahawalpur, Pakistan
[b] Institute of Physics, Faculty of Physical & Mathematical Sciences, The Islamia University of Bahawalpur, Pakistan
[c] Department of Botany, Division of Science and Technology, University of Education, Lahore, Pakistan
[d] Research Center for Eco-Environmental Engineering, Dongguan University of Technology, Dongguan, 523808, China

ARTICLE INFO

Handling Editor: Shivendra Sahi

Keywords:
Cr-mitigation
Osmoprotectants
Oxidative stress and phyto-nanotechnology

ABSTRACT

Chromium (Cr) is a hazardous metal that has a significant risk of transfer from soil to edible parts of food crops, including shoot tissues. Reduction of Cr accumulation is required to lower the risk of Cr-exposed in humans and animals feeding on metal-contaminated parts of such plant. *Zea mays* is a global staple crop irrigated intensively with Cr-contaminated water. Consequently, the objective of this study was to investigate that *FI*-stabilized ZnO NPs could be used as an eco-friendly and efficient amendment to reduced Cr uptake and toxicity in *Zea mays*. To investigate the growth parameters, physiological, oxidative stress and biochemical parameters under different Cr-VI concentrations (10.0, 15.0, and 20.0 ppm). Cr exposed *Z. mays* plants exhibited substantially reduced plant biomass, chlorophyll contents, and altered antioxidant enzyme activity compared to untreated control. The results revealed that foliar application of *Fagonia*-ZnO-NPs helps eliminate the harmful effects of Cr (VI), which can enter plants through soil pollution. Increased levels of proline, soluble sugars and various antioxidant enzymes reflected this. Mean comparisons showed that Cr stress led to a 33–50% reduction in fresh shoot weight, 73–170% in fresh root weight, 16–34% shoot length, 9.5–129% root length, Chlorophyll contents 20–33% (Chl a), 18–27% (Chl b) and 17–27% (car), 14–33% total soluble sugars, 54–170% proline content, 7–7.5% POD, 0.66–75% CAT and 32–77% APX enzyme activities compared to untreated plants. Application of *FI*-stabilized ZnO NPs led to an increase 21–77% in fresh shoot weight, 22–45%, fresh root weight, 3–35% shoot length, 24–154% root length, Chlorophyll contents 39–60% (Chl a), 15–79% (Chl b) and 28–82% (car), 19–52% total soluble sugars, 21–55% proline content, 14–43% POD, 34–95% CAT and 130–186% APX enzyme activities under 10, 15 and 20 ppm Cr stress respectively, compared to Cr-treated plants. However, the principal component analysis revealed that chlorophyll contents, carotenoid, CAT, APX and length were in the same group and showed a positive correlation. These data collectively suggest that phytostabilized zinc oxide NPs may be an eco-friendly solution to mitigate Cr toxicity in agricultural soils and crop plants.

1. Introduction

Globally heavy metal pollution has become a severe environmental hazard in recent decades. Chromium (Cr)VI is a heavy metal found naturally and according to the earth's mantle it is the 17th most abundant element (Bhalerao and Sharma, 2015; Chandra & Kulshrestha, 2004). Although Cr is required at minimal levels for plant and animal growth, it is a serious environmental pollutant at greater concentrations. The emission of Cr(VI) into the soil, air, and water is the result of natural sources and also anthropogenic activities, resulting in Cr(VI) pollution across the world (Lin et al., 2020). Cr quickly penetrates and bioaccumulates directly or indirectly in the food chain due to pollution of food lands and the drinking system (McNeill et al., 2012; Shrivastava et al., 2002; Batayneh, 2012). Plants display indications of Cr(VI) toxicity, including delayed germination of seed, roots damaged and decreased root development, reduced biomass, reduced plant height,

* Corresponding author.
E-mail address: hmadeelcmc@hotmail.com (H.M.Adeel Sharif).

https://doi.org/10.1016/j.plaphy.2023.01.015
Received 12 October 2022; Received in revised form 15 December 2022; Accepted 10 January 2023
Available online 11 January 2023

photosynthetic impairment, membrane damage, leaf chlorosis, necrosis, low grain production, and finally, plant death (Muhammad et al., 2022Amin et al., 2013). In *Triticum. Aestivum*, various Cr(VI) concentrations caused a decrease in root length and root dry weight (Ghani et al., 2015). *Citrus aurantium* is one of these species (Shiyab, 2019), *Najas indica*, *Vallisneria spiralis*, and *Alternanthera sessilis* under Cr(VI) toxicity, there was a reduction in chlorophyll (Chl) concentration (Chandra & Kulshrehtha., 2004). Cr hinders mitochondrial electron transport in higher plants, resulting in raised reactive oxygen species production and oxidative stress, as well as pigment and chloroplast changes (Hauschild and Putrescine., 1993).

Nanotechnology has made enormous strides in the previous two decades in sciences due to its very useful applications in various human welfare domains. Nanoparticles; NPs (1–100 nm) have very strong reactivity, mobility, good surface-to-volume ratio, and numerous distinguished characteristics (Shao et al., 2008; Sharif et al., 2019a). Various plants have been synthesizing an extensive spectrum of metallic NPs (Das et al., 2017; Lin et al., 2020; Adeel et al., 2021). Plants tolerance to heavy metals is significantly enhanced by using NPs, and they can absorb or bind with heavy metals in the soil, limiting the mobility and bioavailability of heavy metals. However, several studies have indicated that plant-mediated AgNPs successfully alleviate salt stress (Abou-Zeid and Ismail, 2018; Almutairi, 2016; Sharif et al., 2019b). Plant-mediated AgNPs were found to assist in preserving water balance in lentils under drought stress by increasing growth parameters such as shoot length, and fresh and dry weight, according to single research (Hojjat, 2016; Banan et al., 2020; Adeel et al., 2021). A previous study reduced cadmium toxicity by applying Moringa zinc oxide (MZnO-NPs) on Linseed plants. Results confirmed that phytostabilized Zn NP can potentially eliminate cadmium negative effects on plant growth (Ramzan et al., 2022). Most NP concentrate in cell walls, bind to heavy metal and render them inactive by creating complexes. These complexes bind to the cell surface and get adsorbed (Wang et al., 2021; Cui et al., 2017), As a result, heavy metal movement in plants is hampered, and their biological activity is reduced. According to the current research, ZnO-NP aids in the reduction of Cr (VI) toxicity by enhancing the activity of the plant's anti-oxidative enzymes.

Furthermore, Zinc (Zn) is an important micronutrient for plant growth and development. Its withdrawal indicators of chlorosis are a reduction in plant vigor. Zn is the only metal found in all six enzymes, making it essential for protein regulation (Bouain et al., 2014; Hafeez et al., 2013).

In the present study, we aimed to investigate the Cr ameliorative potential of ZnO NPs synthesized from *F. indica* leaf via the green method, which is considered low-cost and eco-friendly to the environment. Thus, this research employed *Z. mays* as a model to define the effects of FI-ZnO NPs on seedling growth and its physio-biochemical responses.

2. Materials and methods

2.1. Preparation of Fagonia Indica extract

Fagonia Indica (FI) shrub leaves collected from Lal Sohanra National Park and prepared powder form of washed and dried *Fagonia Indica* leaves. To prepare the broth solution, a 3 g of *FI* (locally known as *Dhaman*) powder was added to 100 ml of distilled water and then heated at 90 °C for 30 min using a hotplate under continuous stirring conditions. After cooling at room temperature, the extract was filtered through Whatman No.1 filter paper to eliminate the residues. The filtrate was stored in a glass vial at 4 °C for further experimentation. As-prepared *FI* green extract was then used for biological reduction and stabilization of ZnO NPs.

2.2. Synthesis of Fagonia Indica-stabilized ZnO nanoparticles

For *FI* extract-mediated synthesis of ZnO NPs, distilled water was used as a solvent throughout the procedure as shown in **schematic 1**. In this typical synthesis, *FI* extract was mixed with 0.5 M zinc acetate dehydrate/$Zn(CH_3CO_2)_2{\cdot}2H_2O$ (Sigma Aldrich, 99.99% purity) solution in a ratio 1:1. The mixture was then put on stirring continuously for 2 h following the dropwise addition of 0.5 M NaOH (Sigma Aldrich, ≥98%, pellets (anhydrous)) solution until resulted in yellowish precipitate formation. The precipitate was then filtered using filter paper and washed twice with distilled water, followed by ethanol to remove the byproducts, and finally, oven-dried at 95 °C for 90 min. The dried cream color powder was fine crushed using a mortar and pestle (Elumalai et al., 2015). After the accompanying thermal stability of the green-synthesized ZnO NPs, the crushed powder sample was calcined at 450 °C for 60 min and fine ground, thus ready for further characterization (see Scheme 1).

3. Characterization

To confirm the morphology and stability of *FI*-stabilized ZnO NPs, the absorption spectrum of the as-prepared sample was obtained through Epoch Microplate Spectrophotometer (UV–Vis) in the 200–800 nm wavelength range. The X-ray diffraction for the sample was performed through Bruker-D8 Advance X-ray Diffractometer with Cu Kα radiation (λ = 1.54 Å), operated at 35 mA and 40 KeV that scanned the sample at room temperature from 20° to 85° for its structural analysis. To examine the surface morphology of *FI*-stabilized ZnO NPs, a JEOL SEM (made in Japan) was used. An X-ray analysis option (EDX) equipped with the SEM was utilized to determine the sample's elemental/quantitative compositional information.

3.1. Experimental design

Maize seeds were obtained from the Poonam Seed Company in Faisalabad. Plastic pots (8 inches) were used to grow the plants. The pots were filled with agricultural (loam) soil and put in a naturally illuminated greenhouse. According to the soil profile, pH is basic (7.9), organic carbon is low (0.38), and Ec is normal (0.18ds meter-1) except for nitrogen and Cr, which are both present in low amounts.

3.2. Treatments

For one month in a shaded region, the soil was spiked with various Cr-treatments (10, 15 and 20 ppm) in the form of $CrCl_2$. The ZnO NPs were prepared in the Physics lab, Islamia University Bahawalpur (IUB), and FI-stabilization. Application of 50 mg/L *FI*-stabilized ZnO NPs was sprayed on one-month-old seedlings of *Zea mays* two times with one weak interval. Applying 50 mg/L FI-stabilized ZnO NPs was sprayed on one-month-old Zea mays seedlings twice with one weak interval. Each treatment was replicated three times. The plants were harvested for further analysis two weeks after the foliar spray.

3.3. Morpho-physiological attributes

Shoot and root length, fresh and dry shoot and root weight, and morphological parameters were measured in cm and gram using a ruler and weighing scale, respectively. Plant tissues were oven dried at 70 °C until they reached a consistent weight.

3.4. Chlorophyll and carotenoid contents

Freshly harvested leaves were used for the concentration of photosynthetic pigments and were measured spectrophotometrically by Lichtenthaler (1987). For Chl "a," Chl "b," and carotenoids, the pigment extract was measured at 663, 644, and 452.5 nm, respectively, against a

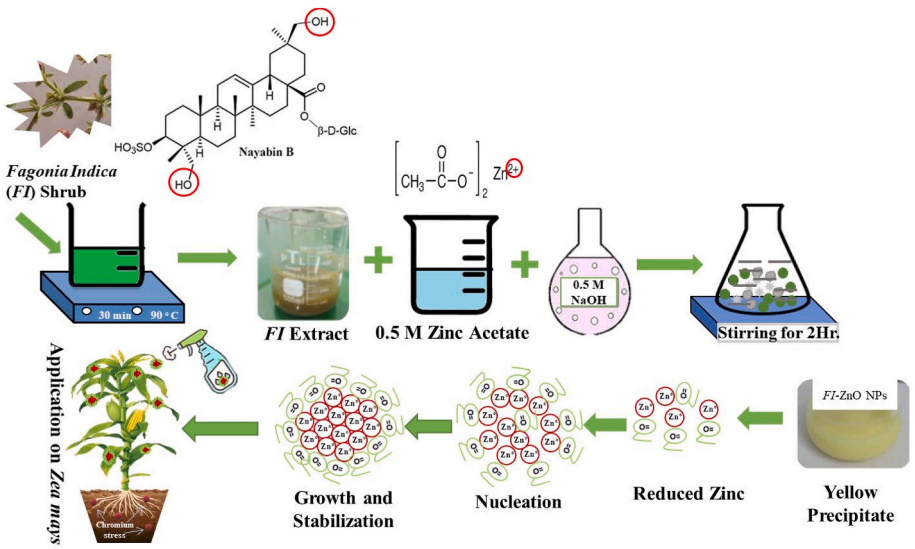

Scheme 1. Schematic illustration of the synthesis of *Fagonia Indica* (*FI*)-stabilized ZnO NPs.

blank of pure 80% acetone.

3.5. Electrolyte leakage

Leaf samples were positioned vertically in a tube of deionized water (10 ml) for 2 h following this, initial electrical conductivity (EC) of the solution was noted (EC_i), then samples were heated for 20 min, cooled, and final EC_f measured. The following formula was used to calculate electrolyte leakage (Dionisio-See and Tobita, 1998).

$$\text{Electrolyte leakage } \% = (Ec_i / Ec_f)\ x \qquad 100$$

3.6. Oxidative stress

Sergiev et al. (1997) set the following protocols, oxidative stress indices such as hydrogen peroxide (H_2O_2) and MDA content of leaves were determined. A spectrophotometer measured the OD at 390 nm, 432 nm, and 600 nm for H_2O_2 and MDA, respectively.

3.7. Osmoprotectants

Bates et al. (1973) provided the methodology for determining proline content, and the optical density was measured with a spectrophotometer at 520 nm. Implementing the methods of (Luo et al., 2008) and (Yem and Willis., 1954), respectively, to estimate total soluble carbohydrates and total soluble protein. The quantity of total protein in the samples was determined using the bovine serum albumin standard curve. At 620 nm, soluble sugar (starch) was spectrophotometrically quantified.

3.8. Estimation of anti-oxidative enzyme activities

The enzyme extraction method was completed at 0–4 °C. Using a previously cold mortar and pestle, 2 g of fresh and cleansed leaf tissue were homogenized in 10 ml of 0.1 M potassium phosphate buffer (pH 7.0). The homogenate was centrifuged for 15 min at 10,000 rpm. The crude extract supernatant was collected and utilized to measure the activity of all the enzymes simultaneously.

3.9. Superoxide dismutase

The activity of SOD to inhibit nitro blue tetrazolium photochemical reduction was assessed using the method of Misra and Fridovich (1972) absorption method at 560 nm.

3.10. Peroxidase

Shannon et al., (1966) method were used to calculate POD enzyme activity. Under assay circumstances. The quantity of enzyme that catalyzed the oxidation process of 1 M H_2O_2 minute^{-1} is defined as one enzyme unit.

3.11. Catalase

The activity of catalase enzymes was assessed using Aebi (1984) technique, and the disappearance of H_2O_2 was measured at 240 nm for 2 min in a UV–Vis spectrophotometer.

3.12. Ascorbate peroxidase

Following the H_2O_2-dependent oxidation of ascorbic acid at 290 nm for 2 min was used to measure enzyme activity (Sairam et al., 2002).

3.13. Statistical analysis

All the data were analyzed using IBM SPSS Statistics 2.3 software, and a One-way analysis of variance and honest significant difference (HSD) test was done. Principal component analysis was also measured by using R software.

4. Results

4.1. Characterization of FI-stabilized ZnO NPs

Fig. 1(a) shows the SEM micrograph taken to evaluate the dimensions and shape of *FI*-stabilized ZnO NPs. The green ZnO NPs are sheet-like structures incorporating small particle sizes in the nano regime. The NPs sample could not be finely ground before the analysis. The size estimate of these small particles falls below 900 nm. Fig. 1(b) shows the corresponding energy dispersive X-ray (EDX) spectroscopic analysis of *FI*-stabilized ZnO NPs, clearly indicating the peaks for Zn and Oxygen. To gain further insight into the composition of *FI*-stabilized ZnO NPs, the analysis of the sample was performed using the dispersive energy X-ray (EDX) spectroscopic technique. The EDX spectrum of the sample obtained from the SEM-EDX analysis shows that the sample

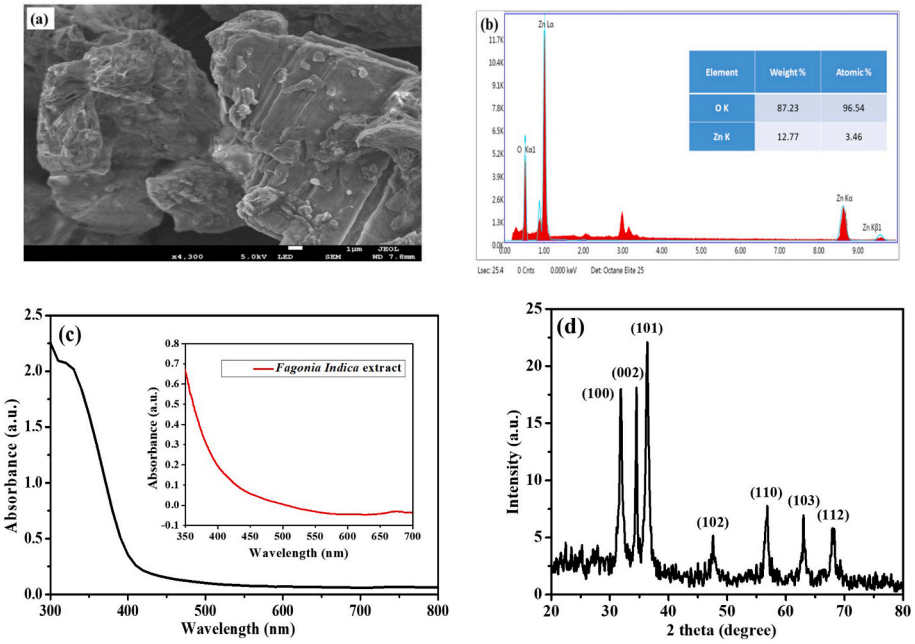

Fig. 1. (a) SEM image of *FI*-stabilized ZnO NPs exhibiting nano size pieces accumulated on the bulk, (b) EDX clearly showing traces of Zn and oxygen, (c) corresponding UV–Vis absorption spectrum and (d) XRD pattern of *FI*- stabilized ZnO NPs.

prepared using *Fagonia Indica* shrub extract has pure ZnO phases, and the reaction product is composed of high-purity ZnO NPs. The approximate atomic ratio of Zn to oxygen was found to be 3.46:96.54, shown by the inset in Fig. 1(b).

Fig. 1(c) shows the UV–Vis absorption spectrum of *FI*-stabilized ZnO NPs. Pure *Fagonia Indica* extract does not show significant absorption in the visible region (Rukhsana Mariam, 2021). Usually, pristine ZnO shows no absorption peak in the visible region, but an equitable absorption band is observed in the UV region, which is attributed to the band edge absorption of the hexagonal wurtzite crystalline structure of ZnO material (Manoj, 2014). Fig. 1(d) shows the XRD pattern of the sample, where the diffraction peaks are obvious at values of 2θ = 31.852°, 34.511°, 36.331°, 47.62°, 56.66°, 62.917°, 66.435°, 67.99°, and 69.175° corresponding to (100), (002), (101), (102), (110), (103), (200), (112), and (201) crystalline planes, respectively. This agrees with the previously reported literature being indexed to the hexagonal wurtzite type of ZnO material (JCPDS 36–1451) (Wang et al., 2020). The sharpness of the XRD pattern reflects the crystalline quality of *FI*- stabilized ZnO NPs. No other diffraction peaks have been observed in the pattern, indicating the absence of any secondary phases of the sample.

The harmful effect of Cr (VI) stress on plant development, chlorophyll content, osmoprotectants, oxidative stress, and antioxidant enzymes was mitigated by *FI*-stabilized ZnO NPs, which resulted in a large increase in their levels. Control plants, *FI*-stabilized ZnO NPs treated plants, and Cr(VI) stressed plants have dramatically different physical appearances. Plants treated with Cr(VI) alone were shorter than those treated with *FI*-stabilized ZnO NPs (50 mg/L). The following are the findings of this research.

4.2. Effect of foliar *FI*-stabilized ZnO NPs on Cr(VI) induced suppression in morphometric parameters

Cr(VI) toxicity reduced plant growth and development as Cr concentrations increased (10, 15, and 20 ppm). The positive influence of exogenously given *FI*-stabilized ZnO NPs on growth characteristics of *Z. mays* plants under Cr(VI) stress was observed. The results demonstrate that under Cr stress, the growth characteristics of *Z. mays* plants significantly deteriorated dramatically compared to control plants ($p < 0.0001$).

4.3. Fresh weight content

In plants cultivated under 10.0, 15.0, and 20.0 ppm Cr, the fresh weight of the shoots reduced by 46%, 33%, and 50%, respectively, compared to control plants (Table .1; Fig. 2). According to the findings, FI-stabilized ZnO NPs considerably boosted the fresh weight content of shoots in Z. mays plants (Fig. 2). Foliar spray of *FI*-stabilized ZnO NPs (50 mg/L) enhanced shoot fresh weight content by 21, 77, and 233.0% under 10.0, 15.0, and 20.0 ppm Cr, respectively.

Cr-treated seedlings (10.0, 15.0, and 20.0 ppm), the fresh weight of the roots was reduced by 73, 98, and 170%, respectively, compared to

Table 1
One-way analysis of variance and honest significant difference (HSD) test values for comparison of eight treatment means of studied variables.

Variables	Mean squares			
	Treatments	Error	F-value	HSD
TSS	3.49	0.015	231.4	0.348
TSP	1.56	0.007	229.2	0.234
Proline	3451.5	0.18	18851.5	1.2
Chl a	0.085	0.00008	1037.37	0.025
Chl b	0.02	0.00002	987.36	0.013
Total Chl	0.18501	0.00007	2613.39	0.024
Carotenoid	0.076	0.00008	957.18	0.025
SOD	874.71	0.005	194,020	0.19
POD	1020.44	0.01	94194.8	0.295
CAT	383.88	0.013	29719.9	0.322
APX	9.68	0.00053	18164.3	0.065
H2O2	3.89	0.00008	46642.1	0.026
MDA	2.45	0.0001	22654.1	0.029
FSW	66.58	0.0006	103,731	0.072
DSW	3.589	0.0018	1994.34	0.12
SDW%	25.23	0.005	4567.33	0.21
Shoot Length	16.49	0.007	2473.99	0.23
EL%	565.83	0.017	32333.5	0.374
FRW	3.44	0.003	1282.35	0.147
DRW	0.155	0.00001	11372.3	0.01
RDW%	2.75	0.09	30.41	0.851
Root length	62.21	0.006	9934.57	0.22

Df for treatment and error is 7 and 16 respectively and effect of eight treatments on each parameter is significant at p-value <0.0001.

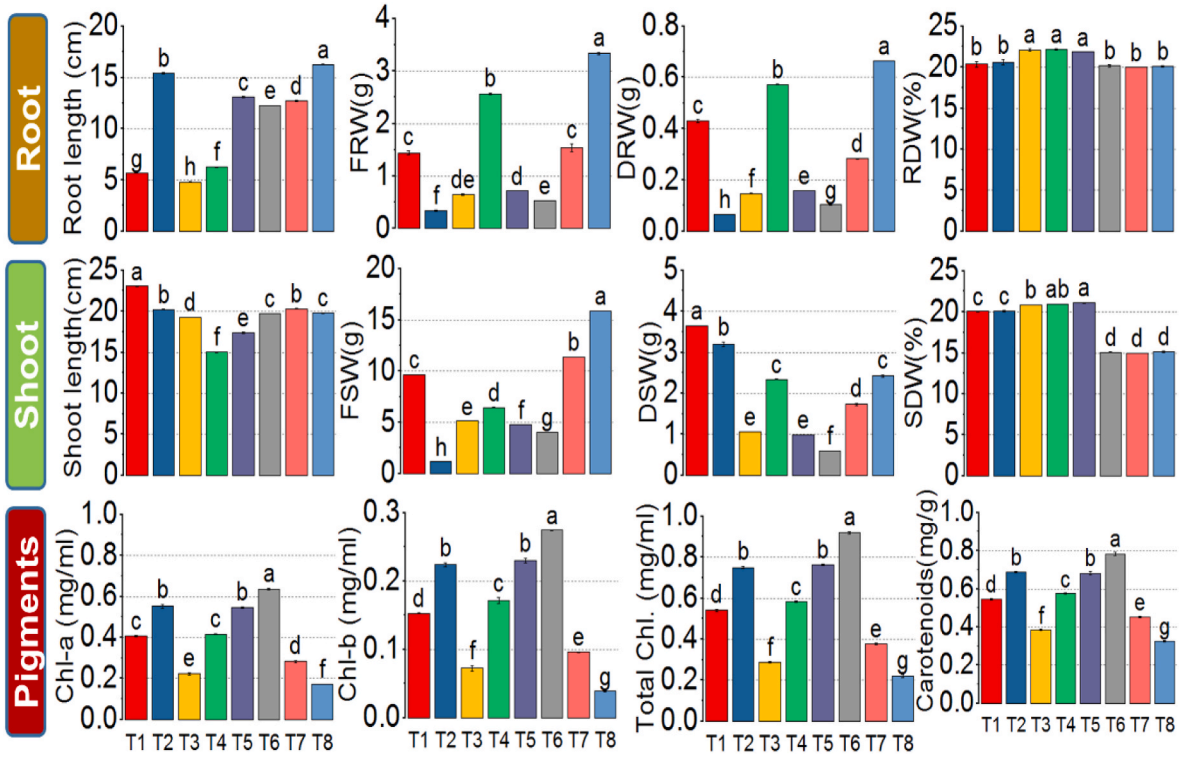

Fig. 2. Treatments of morphological (above) parameters and photosynthetic (below): treatments 1 = control; 2 = 50 mg/L *FI* ZnO NP; 3 = 10 ppm Cr; 4 = 15 ppm Cr; 5 = 20 ppm Cr; 6 = 50 mg/L *FI* ZnO NP +10 ppm Cr; 7 = 50 mg/L *FI* ZnO NP +15 ppm Cr and 8 = 50 mg/L *FI* ZnO NP+ 20 ppm Cr.

control plants (Fig. 2). *Fagonia indica*-ZnO-NP considerably boosted the fresh weight content of roots in *Z. mays* plants, according to the findings (Fig. 2). *FI*-stabilized ZnO NPs supplementation, significant ($p < 0.0001$) increased root fresh weight content was 22%, 45% and 36% in 10.0, 15.0, and 20.0 ppm Cr-treated seedlings, respectively, over Cr-treated seedlings alone (Table-1).

4.4. Dry weight content

Cr (10.0, 15.0, 20.0 ppm) dropped the shoot dry weight by 70.60, 35.98, and 73.46%, respectively, relative to untreated seedlings (Fig. 2). *FI*-stabilized ZnO NPs at 50 mg/L concentrations dramatically raise shoot dry weight in *Z. mays* plants by 54% and 145% at higher levels, viz., 15.0 and 20.0 ppm, except for lower treatment relative to Cr-treated seedlings without NP. Cr-treated plants showed increased root dry weight by 97, 10, and 9.3% at 60 DAS in seedlings cultivated under 10, 15, and 20 ppm Cr, respectively. Exogenous application of 50 mg/L *FI*-stabilized ZnO NPs treatment increased root dry weight by 8, 9, and 7.8% in Cr– treated plants, respectively, relative to Cr-treated plants alone. According to ANOVA (Table .1), F-value was exhibited a significant effect on the dry weight of the plant.

4.5. Shoot and root length

Plants exposed to Cr (10.0, 15.0, and 20.0 ppm) had decreased shoot length by 16.52, 34.34, and 23.91%, respectively, compared to non-Cr-treated plants. Exogenous administration of 50 mg/L *FI*-stabilized ZnO NPs increased shoot length by 10.0, 15.0, and 20.0 ppm Cr-exposed plants by 3.12, 35, and 13%, respectively, relative to the plants treated with Cr without *FI*-stabilized ZnO NPs. (Fig. 2).

Plants exposed to Cr (10.0, 15.0, and 20.0 ppm) had decreased root length by 15.19, 9.54, and 129.68%, respectively, compared to non-Cr-treated plants. Exogenous administration of 50 mg/L *FI*-stabilized ZnO NPs increased root length by 10.0, 15.0, and 20.0 ppm Cr-exposed plants by 154.1, 106.45, and 24%, respectively, relative to the plants treated with Cr without *FI*-stabilized ZnO NPs (Fig. 2). According to ANOVA (Table .1), F-value exhibited significant effects on shoot and root length.

4.6. Chlorophyll contents

Chlorophyll “a” and “b” contents decreased by 25, 33, and 20% (Figs. 2) and 31, 18, and 27% in *Z. mays* plants grown under 10, 15, and 20 ppm Cr, correspondingly. *FI*-stabilized ZnO NPs (50 mg/L) considerably boosted the chlorophyll contents in Cr-treated *Z. mays* plants. Plants cultivated less than 10 ppm, 15 ppm, and 20 ppm Cr increased their chlorophyll “a" content by 60, 55, and 39% at 60 DAS on 50 mg/L *FI*-stabilized ZnO NPs treatment. At 60 DAS, *FI*-stabilized ZnO NPs (50 mg/L) improved the chlorophyll “b" content of plants growing under 10.0 ppm, 15.0 ppm, and 20.0 ppm Cr by 79.3, 43.3 and 15.69%, respectively. Carotenoids increased by 43.4, 82.5 and 28.71% at 60 DAS in plants cultivated under 10.0 ppm, 15.0 ppm, and 20.0 ppm Cr, respectively, after treatment with 50 mg/L *FI*-stabilized ZnO NPs. Furthermore, in 10.0, 15.0, and 20.0 ppm Cr-treated plants, carotenoid levels decreased by 27, 17, and 21%, respectively. According to ANOVA (Table .1), F-value exhibited a significant difference between all treatments based on photosynthetic parameters.

5. Oxidative stress and electrolyte leakage

Plants exposed to Cr (10.0, 15.0, and 20.0 ppm) had increased H_2O_2 levels by 65.11, 17.44, and 277%, respectively, compared to non-Cr-treated plants. Exogenous administration of 50 mg/L *FI*-stabilized ZnO NPs reduced MDA content in combination with 10.0, 15.0, and 20.0 ppm Cr-exposed plants by 55.63, 5, and 17.23%, respectively, relative to the plants treated with Cr without *FI*-stabilized ZnO NPs (Fig. 3).

Plants exposed to Cr (10.0, 15.0, and 20.0 ppm) had increased MDA levels by 17.27, 4.54, and 96%, respectively, compared to non-Cr-treated plants. Exogenous administration of 50 mg/L *FI*-stabilized ZnO NPs reduced MDA with 10.0, 15.0, and 20.0 ppm Cr-exposed plants by 29.06, 6.66, and 9.22%, respectively, relative to the plants treated with

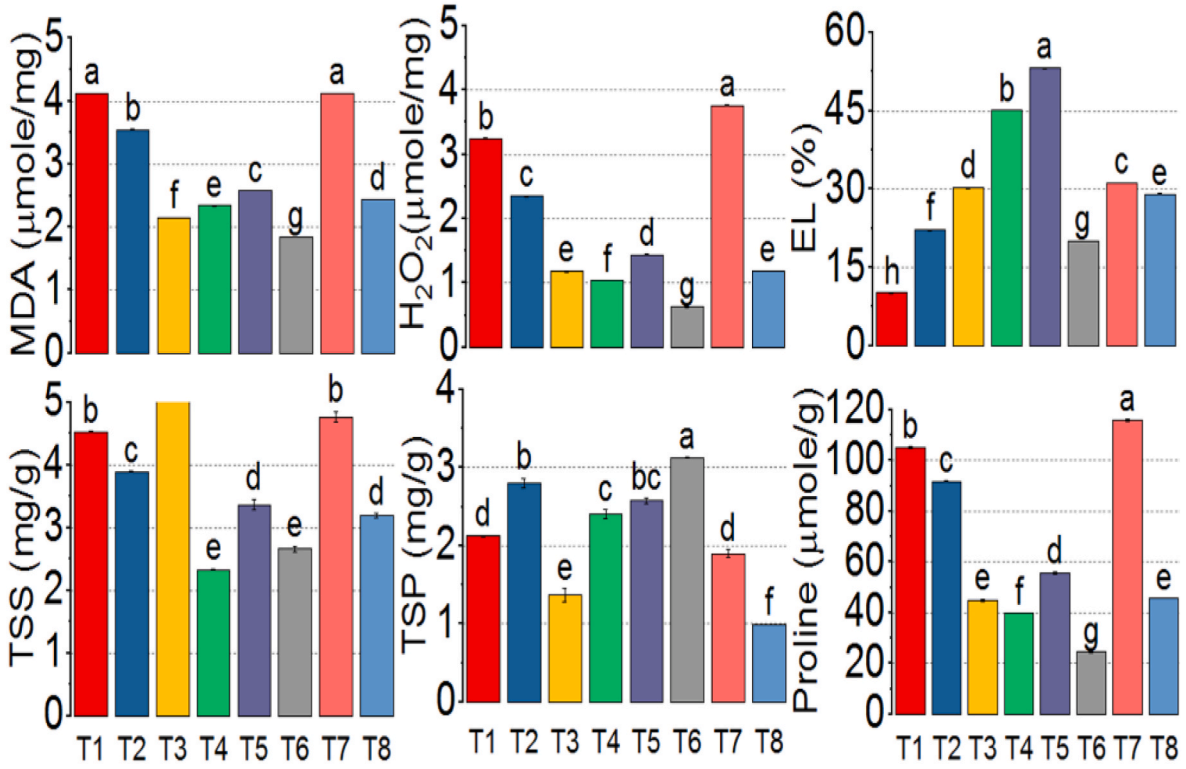

Fig. 3. Parameters of Oxidative (above) and Osmotic (below): treatments 1 = control; 2 = 50 mg/L *FI* ZnO NP; 3 = 10 ppm Cr; 4 = 15 ppm Cr; 5 = 20 ppm Cr; 6 = 50 mg/L *FI* ZnO NP +10 ppm Cr; 7 = 50 mg/L *FI* ZnO NP +15 ppm Cr and 8 = 50 mg/L *FI* ZnO NP+ 20 ppm Cr.

Cr without *FI*-stabilized ZnO NPs (Fig. 3).

Plants exposed to Cr (10.0, 15.0, and 20.0 ppm) had increased electrolyte leakage by 200, 350, and 430%, respectively, compared to non-Cr-treated plants. Exogenous administration of 50 mg/L *FI*-stabilized ZnO NPs reduced electrolyte leakage in the 10.0, 15.0, and 20.0 ppm Cr-exposed plants by 33.33, 31.11, and 45.28%, respectively, relative to the plants treated with Cr without *FI*-stabilized ZnO NPs (Fig. 3).

6. Total soluble sugars, protein and proline

For plants exposed to 10.0, 15.0, and 20.0 ppm Cr, the amount of soluble sugar fell by 33.89, 14.22, and 15.89%, respectively, compared to the non-Cr-treated plants. However, foliar spray of 50 mg/L *FI*-stabilized ZnO NPs improved total soluble sugar by 19.06, 46.52, and 52.70%, respectively, relative to their respective negative controls.

Plants exposed to Cr (10.0, 15.0, and 20.0 ppm) had reduced total soluble protein content by 200, 250, and 350%, respectively, compared to non-Cr-treated plants. Exogenous administration of 50 mg/L *FI*-stabilized ZnO NPs raised total soluble protein concentration in combination with 10.0, 15.0, and 20.0 ppm Cr-stressed plants by 91.95, 94.91, and 64.63%, respectively, as compared to the plants treated with Cr alone (Fig. 3).

Plants exposed to Cr (10.0, 15.0, and 20.0 ppm) had reduced proline content by 170, 54.15, and 63.69%, respectively, compared to non-Cr-treated plants. Exogenous administration of 50 mg/L *FI*-stabilized ZnO NPs raised proline concentration in the 10.0, 15.0, and 20.0 ppm Cr-stressed plants by 55.63, 219, and 21.28%, respectively, as compared to the plants treated with Cr alone. Table .1 shows that significant differences among treatments were observed for oxidative stress parameters.

6.1. Effect of Cr(VI) and exogenous FI-stabilized ZnO NPs on anti-oxidative defense system of Z.mays plants

The activity of Superoxide dismutase increased by 221–431%, but the activities of peroxidase, catalase, and ascorbate peroxidase enzymes decreased by 7.0–7.56, 0.66–75.25%, and 32.48–77.69%, respectively, as the concentration of Cr (10.0, 15.0, and 20.0 ppm) (Fig. 4). In comparison to Cr-treated *Z. mays* plants alone, *FI*-stabilized ZnO NPs (50 mg/L) treatment with Cr concentrations (10.0, 15.0, and 20.0 ppm) boosted SOD (108–277%), POD (14.75–43.0%), CAT (34.88–95.77%), and APX (130–186%) enzyme activity.

6.2. Effect of exogenous FI-stabilized ZnO NPs on Cr-VI accumulation in Z.mays plant

With an increase in Cr(VI) supply, the Cr(VI) concentration in *Z. mays* roots increased dramatically (3–7%). Cr(VI) content in *Z. mays* roots rose as the growth stage progressed. Exogenous application of *FI*-stabilized ZnO NPs (50 mg/L) resulted in a significant reduction (4–10%) in Cr(VI) absorption from the soil to the roots of *Z. mays* (**Supplementary,** Fig. 1). Applying *FI*-stabilized ZnO NPs to *Z. mays* plants cultivated under Cr stress reduced its toxicity considerably.

6.3. Principal component analysis

Principal component analysis (PCA) was performed on the studied variables and their eight treatments as observations. Through eigenvalue analysis, seven principal components (PCs) were generated, explaining 100% variation under the eigenvalue up to 0.192. The principal component at the x-axis (PC1) was extracted with an eigenvalue of 10.546, explaining 48% variation. The principal component at the y-axis (PC2) with 4.026 eigenvalues captured 18% of variation; hence 66% variation in the data was explained by this PCA. Chlorophyll contents, chlorophyll *a*, carotenoid, CAT, APX, and Length were

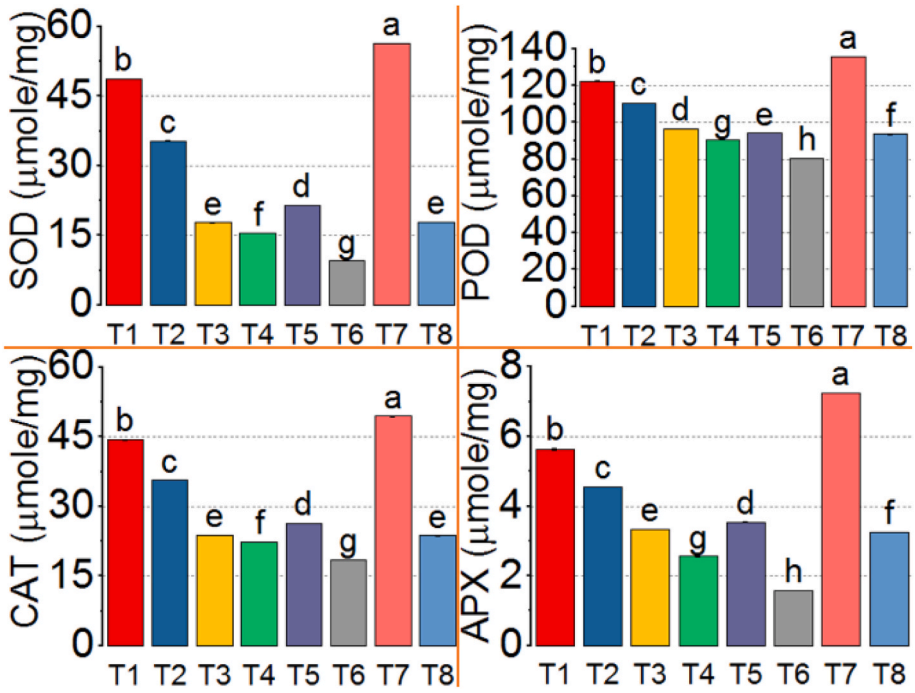

Fig. 4. Antioxidant enzymes viz, superoxide dismutase (SOD); peroxidase dismutase (POD); catalase (CAT) and ascorbic peroxidase (APX): treatments 1 = control; 2 = 50 mg/L *FI* ZnO NP; 3 = 10 ppm Cr; 4 = 15 ppm Cr; 5 = 20 ppm Cr; 6 = 50 mg/L *FI* ZnO NP +10 ppm Cr; 7 = 50 mg/L *FI* ZnO NP +15 ppm Cr and 8 = 50 mg/L *FI* ZnO NP+ 20 ppm Cr.

explained by the PC1 and grouped under positive correlation (Table 2 (Supplementary), Fig. 5-right); while TSP, SDW% and EL% were placed in negative correlation to the PC1. At PC2, TSS, proline, POD, H_2O_2, MDA, EL%, FRW, and DRW were explained with high eigenvector values.

Treatments as observations were also grouped based on the strength of association using PCA. Treatment of 10.0, 15.0, and 20.0 ppm Cr grouped along PC1 and were negatively correlated with 50 and 50 + 15.0 GNP treatments at the x-axis (PC1). Treatment of 50 GNP+20.0 Cr was explained by PC2 and negatively correlated with control and *FI*-stabilized ZnO NPs +10.0 Cr along the y-axis (Fig. 5 left).

7. Discussion

In agricultural soils worldwide, Cr poisoning has become a serious concern and needs to be addressed immediately (Maiti et al., 2014; Pandey et al., 2009). Cr(VI) contamination has had several harmful consequences on the health of plants and animals (Ali et al., 2015). By interfering with various biochemical and physiological processes, Cr (VI) prevents seed germination and plant development, including protein synthesis, photosynthesis, and the enzymatic and non-enzymatic anti-oxidative defense system (Farooq et al., 2016; Li et al., 2005). Plant quality and tolerance capacity are also affected by Cr(VI) toxicity (Atici et al., 2005; Shao et al., 2008). The present study exogenously supplied *FI*-stabilized ZnO NPs, and was used to investigate their ameliorative function in *Z. mays* plants treated with various Cr concentrations (10.0, 15.0, and 20.0 ppm). The conclusions of this study agree with the findings of other researchers who revealed that phytostabilized NPs positively reduced Cr toxicity in different plant species (Mingshu et al., 2021; Patnaik et al., 2013). Present results confirmed that Cr (VI) levels increased in different plant parts when Cr (VI) levels increased in the soil. Numerous researchers observed similar findings in

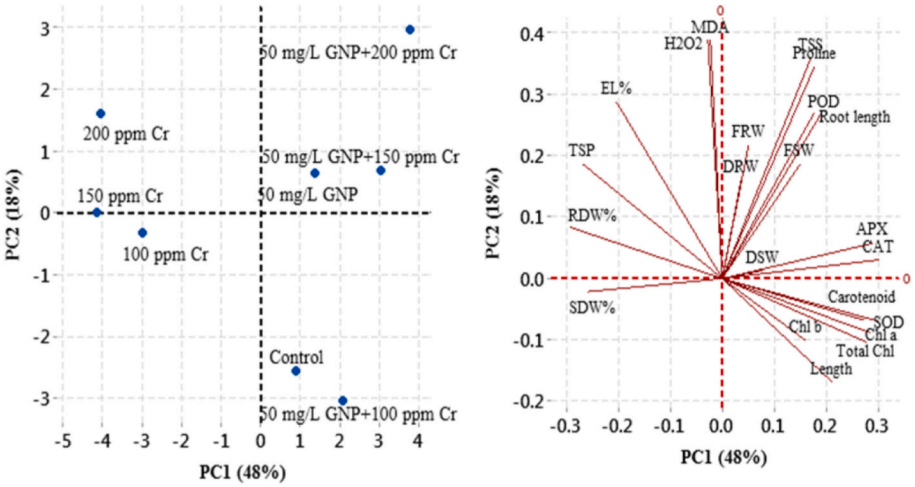

Fig. 5. Principal component analysis (PCA) of studied treatments (left) and variables (right).

mung bean plants cultivated under Cr stress (Banerjee et al., 2011; Bera et al., 1999; Samantaray, 2002). Similar findings were observed by Gomes et al. (2001).

Applying NPs to a plant can result in the modification of gene expression and alteration of genetic pathways, ultimately affecting the growth and development of that plant (Adeel et al., 2021; Nair et al., 2010). In a recent study (Abdelsalam et al., 2019), the effect of foliar-applied NPs was studied. AgNPs have been shown to interfere with nitrification activity and possibly affect nitrogen oxide emissions (Ahmad et al., 2019; Zheng et al., 2017).

Through co-precipitation, iron oxide NPs from leaf extract could stabilize Cd and As in soil (Lin et al., 2019; Su et al., 2020). In a roundabout way, green NPs can help with soil cleanup. Plant extract-mediated Ag NPs may help plants grow by increasing soil pH, nutritional bioavailability, and water retention capacity (Das et al., 2017; Sharif et al., 2023).

The current investigation found that 20.00 ppm Cr significantly lowered the chlorophyll content in maize plants (Figs. 1–2). However, using *FI*-stabilized ZnO NPs (50 mg/L) considerably boosted total chlorophyll content (27–65.64%). *FI*-stabilized ZnO NPs treatment at 50 mg/L in maize plants resulted in the greatest increase. The photosynthetic pigments were changed by *FI*-stabilized ZnO NPs application, which increased plant performance such as nutrition intake and anti-oxidative defense. It is also known that metal ions influence the activity of the photosystem and, thus, the course of photosynthesis (Wiechen et al., 2012). Silver ions released from AgNPs can be expected to subsequently interfere with these key metabolic pathways (Karel et al., 2019). As compared to control plants, *FI*-stabilized ZnO NPs (50 mg/L) considerably improved plant growth (root-shoot length) of maize under Cr (VI) toxicity (3.12–154.1%). (Fig. 1).

Seedlings treated with green-synthesized NPs had longer root and shoot lengths (47% root and 105% shoot) than those treated with chemical ZnO NPs at 62.0 mg/L concentrations. At different NP levels (0, 15, 62, 125, 250, and 500 mg/L), the optimal concentrations of ZnO NPs for seedling emergence and germination of wheat (*Triticum aestivum* L.) were investigated. As a result, the green ZnO NP-treated seeds grew faster than the control seeds (Singh et al., 2019). In the study of (Prasad and Jha, 2009), even a small dose of GNPs greatly impacted the growth and production rate of peanut seeds. The particle size, distribution, chemical content, surface properties, and NP application level have all been found to affect plant germination growth (Noman et al., 2022; Xiang et al., 2015; Zafar et al., 2016; Jhansi et al., 2017).

Protein contains a high amount of proline, an essential amino acid. During times of stress, free proline is extremely important in plants. Under physiological and pathological stress situations, many studies have revealed a significant increase in proline content. In the current study, *FI*-stabilized ZnO NPs were found to increase proline, soluble carbohydrates, and total soluble protein levels (Fig. 3) under different Cr (VI) treatments, implying that green NP may protect against heavy metal stress.

Plants can use enzymes like ascorbate peroxidase, catalase, superoxide dismutase, polyphenol oxidase, peroxidase, and glutathione reductase, to defend themselves from the detrimental effects of heavy metal stress and metabolites like glutathione, proline, and ascorbate to reduce reactive oxygen species (ROS) accumulation (Shahid et al., 2014; Singh et al., 2013). According to the findings, the *FI*-stabilized ZnO NPs treatment (50 mg/L) boosted the activity of antioxidant enzymes in maize plants cultivated under Cr stress (Fig. 4). Compared to control and Cr(VI) treated plants, *FI*-stabilized ZnO NPs treatment significantly boosted superoxide dismutase, peroxidase, ascorbate peroxidase, and catalase enzyme activity (27.89–344%). According to reports, ascorbate and proline may consume ROS produced in plants due to stress (Akram et al., 2017; Hayat et al., 2012). By quenching or converting ROS into safe forms, the anti-oxidative defense system (enzymatic and non-enzymatic) may protect plant cells from oxidative damage (Karel et al., 2019). The administration of *FI*-stabilized ZnO NPs during Cr stress improved the activity of all anti-oxidative enzymes in this investigation.

Furthermore, chronic Cr stress reduces the capacity of maize plants' anti-oxidative defense mechanism to withstand Cr stress. Because the anti-oxidative defense mechanism in Cr-treated plants is less active, antioxidants are less effective at consuming ROS, increasing the likelihood of ROS accumulation in the plant cell, which leads to plant mortality. However, foliar spray of plant-mediated NPs boosted the anti-oxidative defense system's activity, and efficiency in certain plants (under 10.0, 15.0, and 20.0 ppm of Cr treatment alone), resulting in reduced stressed conditions enhanced growth and quality metrics due to decreased Cr buildup and excess ROS. It suggested that *FI*-stabilized ZnO NPs have anti-toxicity properties concerning Cr toxicity. Increases in plant height, root length, chlorophyll content, and quality indices were observed in this study, which could be attributed to *FI*-stabilized ZnO NPs -induced decreases in Cr uptake in plants and increased activity of antioxidant enzymes and osmoprotectants.

8. Conclusion

In this study, we explored the impact of *FI*-stabilized ZnO NPs on the morpho-physiological and biochemical parameters of maize under Cr stress. A low dose of *FI* ZnO NPs improved plant growth under Cr-stress by alleviating oxidative stress and regulating the biochemical attributes in *Z. mays* plants caused by Cr. Biogenic ZnO NP effectively decreased the Cr content in plants and increased the plant biomass. Notably, only a low dose of NPs could significantly increase the fresh weight of shoot and roots, length of shoot and roots of *Z. mays* plants. The photosynthetic parameters in NP-treated plants increased considerably. Furthermore, *FI*-stabilized ZnO NPs significantly increased the SOD, POD, CAT and APX enzymes. The results provide a basis for understanding the effect of *FI*-stabilized ZnO NPs on heavy metals; however, the modification and repair mechanisms need to be further explored.

Author contributions statement

Musarrat Ramzan: Conceptualization, Methodology, Investigation, Data curation, Writing - original draft. **Gul Naz:** Writing - review & editing, Software, Data curation, Writing - original draft. **Anis Ali shah:** Writing - review & editing and provided statistical data experimental data. **Misbah Parveen:** Investigation, Data curation, Software, Writing - original draft. **Muhammad Jamil:** Writing - review & editing, Validation, Investigation. **Sidra Gill:** Writing - review & editing and provided statistical data experimental data. **Hafiz M. Adeel Sharif:** Funding acquisition, Writing - review & editing, Supervision, Project administration.

Declaration of competing interest

The authors declare that they have no known competing financial interests or personal relationships that could have appeared to influence the work reported in this paper.

Data availability

Data will be made available on request.

Acknowledgements

This study was supported by the National Natural Science Foundation of China (Grant No. 22050410268).

Appendix A. Supplementary data

Supplementary data to this article can be found online at https://doi.org/10.1016/j.plaphy.2023.01.015.

References

Adeel, M., Noman, S., Tariq, H., Imran, A., Pingfan, Z., Peng, Z., Yi, H., Jorg, R., Yukui, R., 2021. Bio interaction of bulk and nano lanthanum and ytterbium oxides in soil system: biochemical, genetic and histopathological effects on Eisenia fetida. J. Hazard Mater. 415, 125574.

Ahmad, M.A., Yuesuo, Y., Ao, Q., Adeel, M., Hui, Z.Y., Javed, R., 2019. Appraisal of comparative therapeutic potential of undoped and nitrogen-doped titanium dioxide nanoparticles. Molecules 24, 3916. https://doi.org/10.3390/molecules24213916.

Abdelsalam, N.R., Kandil, E.E., Al-Msari, M.A.F., Al-Jaddadi, M.A.M., Ali, H.M., Salem, M.Z.M., Elshikh, M.S., 2019. Effect of foliar application of NPK nanoparticle fertilization on yield and genotoxicity in wheat (*Triticum aestivum* L.). Sci. Total Environ. 653, 1128–1139 ([CrossRef]).

Abou zeid, H., Ismail, G., 2018. The role of priming with biosynthesized silver nanoparticles in the response of *Triticum aestivum* L. to salt stress. Ejypt, J.Bot 58, 73–85.

Aebi, H., 1984. Catalase in vitro. Methods Enzymol. 105, 121–126.

Akram, N.A., Shafiq, F., Ashraf, M., 2017. Ascorbic acid-A potential oxidant scavenger and its role in plant development and abiotic stress tolerance. Front. Plant Sci. 8, 613.

Ali, S., et al., 2015. Alleviation of chromium toxicity by glycine betaine is related to elevated antioxidant enzymes and suppressed chromium uptake and oxidative stress in wheat (*Triticum aestivum* L.). Environ. Sci. Pollut. Res. 22, 10669–10678.

Almutairi, Z.M., 2016. Influence of silver nano-particles on the salt resistance of tomato (*Solanum lycopersicum*) during germination. Int. J. Agric. Biol. 18, 449–556.

Amin, H., Arain, B.A., Amin, F., Surhio, M.A., 2013. Phytotoxicity of chromium on germination, growth and biochemical at-tributes of *Hibiscus esculentus* L. Am. J. Plant Sci. 4, 41293 ([CrossRef]).

Atici, O., Agar, G., Battal, P., 2005. Changes in phytohormone contents in chickpea seeds germinating under lead or zinc stress. Biol. Plant. (Prague) 49, 215–222.

Banan, A., Kalbassi, M.R., Bahmani, M., Sotoudeh, E., Johari, S.A., Jonathan, M.A., Kolok, A.S., 2020. Salinity modulates biochemical and histopathological changes caused by silver nanoparticles in juvenile Persian sturgeon (*Acipenser persicus*). Environ. Sci. Pollut. Res. 27, 10671–10678.

Banerjee, S., Datta, S., Chattyopadhyay, D., Sarkar, P., 2011. Arsenic accumulating and transforming bacteria isolated from contaminated soil for potential use in bioremediation. J. Environ. Sci. Health. A. 46, 1736–1747.

Batayneh, A.T., 2012. Toxic (aluminum, beryllium, boron, chromium and zinc) in groundwater: health risk assessment. Int. J. Environ. Sci. Technol. 9, 153–162 ([CrossRef]).

Bera, A.K., Bokaria, K., 1999. Effect of tannery effluent on seed germination, seedling growth and chloroplast pigment content in mungbean (*Vigna radiata* L. Wilczek). Environ. Ecol. 17, 35–37.

Bhalerao, S.A., Sharma, A.S., 2015. Chromium: as an environmental pollutant. Int. J. Curr. Microbiol. Appl. Sci. 4, 732–746.

Chandra, P., Kulshreshtha, K., 2004. Chromium accumulation and toxicity in aquatic vascular plants. Bot. Rev. 70, 313–327 ([CrossRef]).

Cui, J., Liu, T., Li, F., Yi, J., Liu, C., Yu, H., 2017. Silica nanoparticles alleviate cadmium toxicity in rice cells: mechanisms and size effects. Environ. Pollut. 228, 363–369.

Das, R.K., Pachapur, V.L., Lonappan, L., Naghdi, M., Pulicharla, R., Maiti, S., Cledon, M., Dalila, L.M.A., Sarma, S.J., Brar, S.K., 2017. Biological synthesis of metallic nanoparticles: plants, animals and microbial aspects. Nanotechnol. Environ. Eng. 2, 1–21 ([CrossRef]).

Dionisio -See, M.L., Tobita, S., 1998. Antioxidant responses of rice seedlings to salinity stress. Plant Sci. 135, 1–9.

Farooq, M.A., et al., 2016. Cadmium stress in cotton seedlings: physiological, photosynthesis and oxidative damages alleviated by glycinebetaine. South Afr. J. Bot. 104, 61–68.

Ghani, A., Khan, I., Umer, S., Ahmed, I., Mustafa, I., Mohammad, N., 2015. Response of wheat (*Triticum aestivum*) to exog-enously applied chromium: effect on growth, chlorophyll and mineral composition. J. Environ. Anal. Toxicol. 5 ([CrossRef]).

Gomes, P.C., et al., 2001. Selectivity sequence and competitive adsorption of heavy metals by Brazilian soils. Soil Sci. Soc. Am. J. 65, 1115–1121.

Hauschild, M., 1993. Putrescine (1,4-diaminobutane) as an indicator of pollution-induced stress in higher plants: barley and rape stressed with Cr(III) or Cr(VI). Ecotoxicol. Environ. Saf. 26, 228–247 ([CrossRef]).

Hayat, S., et al., 2012. Role of proline under changing environments: a review. Plant Signal. Behav. 7, 1456–1466, 2012.

Hojjat, S.S., 2016. The effect of silver nanoparticle on lentil seed germination under drought stress. Int. J. Farming Allied Sci. 5, 208–212.

Jhansi, K., Jayarambabu, N., Reddy, K.P., Reddy, N.M., Suvarna, R.P., Rao, K.V., Rajendar, V., 2017. Biosynthesis of MgO nanoparticles using mushroom extract: effect on peanut (*Arachis hypogaea L.*) seed germination. Biotech 7 (4), 1–11.

Karel, S., Bozena, H., Michaela, D., Martina, S., Dagmar, U., Zuzana, T., Marta, K., Halina, M., Carlos, F., Branislav, R.N., Hoai, V.N., Augustine, O., Jiri, S., Rene, K., 2019. An assessment of the effect of green synthesized silver nanoparticles using sage leaves (*Salvia officinalis* L.) on germinated plants of maize (*Zea mays* L.). Nanomaterials 9, 1550. https://doi.org/10.3390/nano9111550.

Li, W., Khan, M.A., Yamaguchi, S., Kamiya, Y., 2005. Effects of heavy metals on seed germination and early seedling growth of *Arabidopsis thaliana*. Plant Growth Regul. 46, 45–50.

Lichtenthaler, H.K., 1987. Chlorophylls and carotenoids: pigments of photosynthetic biomembranes. Methods Enzymol. 148, 350–382.

Lin, J., He, F., Su, B., Sun, M., Owens, G., Chen, Z., 2019. The stabilizing mechanism of cadmium in contaminated soil using green synthesized iron oxide nanoparticles under long-term incubation. J. Hazard Mater. 379, 120832 ([CrossRef]).

Lin, -J.P., Muhammed, A., Noman, S., Ke-Rui, G., Dai-Fu, M., Muhammad, A.A., Guo, -Q. L., Mei, -H.Z., Sheng, -E.L., Yu, -K.R., 2020. Engineered nanomaterials suppress the soft rot disease (*Rhizopus stolonifer*) and slow down the loss of nutrient in sweet potato. Nanomaterials 11, 2572.

Maiti, S., et al., 2014. Responses of the maize plant to chromium stress with reference to antioxidation activity. Braz. J. Plant Physiol. 24, 203–212.

McNeill, L., McLean, J., Edwards, M., Parks, J., 2012. State of the science of hexavalent chromium in drinking water. Water Res. 44, 50.

Mingshu, L., Peng, Z., Muhammad, A., Zhiling, G., Andrew, J., Chetwynd, C.M., Tonghao, B., Yi, H., Yukui, R., 2021. Physiological impacts of zero valent iron, Fe3O4 and Fe2O3 nanoparticles in rice plants and their potential as Fe fertilizers. Environ. Pollut. 269, 116134, 0269-7491.

Misra, H.P., Fridovich, I., 1972. The role of superoxide anion in the autoxidation of epinephrine and a simple assay for superoxide dismutase. J. Biol. Chem. 247, 3170–3175.

Nair, R., Varghese, S.H., Nair, B.G., Maekawa, T., Yoshida, Y., Kumar, D.S., 2010. Nanoparticulate material delivery to plants. Plant Sci. 179, 154–163 ([CrossRef]).

Noman, S., Muhammad, A., Muhammad, Z., Peng, Z., Muhammad, A.A., Tahir, F., Pingfan, Z., Imran, A., Muhammad, R., Kerui, G., Ghulam, J., Sunny, A., Saliha, M., Xu, M., Yukui, R., 2022. Exposure of cherry radish (*Raphanus sativus* L. *var. Radculus Pers*) to iron-based nanoparticles enhances its nutritional quality by trigging the essential elements. Nanoimpact 25, 100388.

Pandey, V., Dixit, V., Shyam, R., 2009. Chromium effect on ROS generation and detoxification in pea (Pisum sativum) leaf chloroplasts. Protoplasma 236, 85–95.

Patnaik, A.R., Achary, V.M.M., Panda, B.B., 2013. Chromium (VI)-induced hormesis and genotoxicity are mediated through oxidative stress in root cells of *Allium cepa* L. Plant Growth Regul. 71, 157–170.

Prasad, K., Jha, A.K., 2009. ZnO nanoparticles: synthesis and adsorption study. Nat. Sci. 1, 129, 02.

Ramzan, M., Ayub, F., Shah, A.A., Naz, G., Shah, A.N., Malik, A., Abd-Elgawad, H., 2022. Synergistic effect of Zinc oxide nanoparticles and Moringa oleifera leaf extract Alleviates cadmium toxicity in *Linum usitatissimum*: antioxidants and Physiochemical studies. Front. Plant Sci. 13.

Sairam, R.K., Rao, K.V., Srivastava, G.C., 2002. Differential response of Wheat genotypes to long term salinity stress in relation to oxidative stress, antioxidant activity and osmolyte concentration. Plant Sci. 163, 1037–1046.

Samantaray, S., 2002. Biochemical responses of Cr-tolerant and Cr-sensitive mung bean cultivars grown on varying levels of chromium. Chemosphere 47, 1065–1072.

Sergiev, L., Alexieva, V., Karanov, E., 1997. Effect of spermine, atrazine and combination between them on some endogenous protective systems and stress markers in plants. C. R. Acad. Sci. 51, 121–124.

Shahid, M., et al., 2014. Heavy metal-induced reactive oxygen species: phytotoxicity and physicochemical changes in plants. Rev. Environ. Contam. Toxicol. 232, 1–44.

Shao, H., Chu, L., Shao, M., Jaleel, C.A., Hong-mei, M., 2008. Higher plant antioxidants and redox signaling under environmental stresses. C. R. Biol. 331, 433–441.

Sharif, H.M.A., Cheng, H.-Y., Haider, M.R., Khan, K., Yang, L., Wang, A.-J., 2019a. NO removal with efficient recovery of N_2O by using recyclable Fe3O4@EDTA@Fe(II) complex: a novel approach toward resource recovery from flue gas. Environ. Sci. Technol. 53 (2), 1004–1013 ([CrossRef]).

Sharif, H.M.A., Mahmood, A., Cheng, H.-Y., Djellabi, R., Ali, J., Jiang, W.-L., Wang, S.-S., Haider, M.R., Mahmood, N., Wang, A.-J., 2019b. Fe3O4 nanoparticles coated with EDTA and Ag nanoparticles for the catalytic reduction of organic dyes from wastewater. ACS Appl. Nano Mater. 2 (8), 5310–5319 ([CrossRef]).

Sharif, H.M.A., Asif, M.B., Wang, Y., Hou, Y.-N., Yang, B., Xiao, X., Li, C., 2023. Spontaneous intra-electron transfer within rGO@Fe2O3-MnO catalyst promotes long-term NOx reduction at ambient conditions. J. Hazard Mater. 441, 129951 ([CrossRef]).

Shiyab, S., 2019. Morphophysiological effects of chromium in sour orange (*Citrus aurantium* L.). Hortscience 54, 829–834 ([CrossRef]).

Shrivastava, R., Upreti, R.K., Seth, P.K., Chaturvedi, U.C., 2002. Effects of chromium on the immune sys-tem. FEMS Immunol. Med. Microbiol. 34, 1–7 ([CrossRef]).

Singh, H.P., Mahajan, P., Kaur, S., Batish, D.R., Kohli, R.K., 2013. Chromium toxicity and tolerance in plants. Environ. Chem. Lett. 11, 229–254.

Singh, J., Kumar, S., Alok, A., Upadhyay, S.K., Rawat, M., Tsang, D.C., Kim, K.H., 2019. The potential of green synthesized zinc oxide nanoparticles as nutrient source for plant growth. J. Clean. Prod. 214, 1061–1070.

Wang, A., Jin, Q., Xu, X., Miao, A., White, J.C., Gardea-Torresday, J.L., Ji, R., Zhao, L., 2020. High-Throughput screening for engineered nanoparticles that enhances photosynthesis using mesophyll protoplasts. J. Agric. Food Chem. 68, 3382–3389.

Wang, K., Wang, Y., Wan, Y., Mi, Z., Wang, Q., Wang, Q., Li, H., 2021a. The fate of arsenic in rice plants (*Oryza sativa* L.): influence of different forms of selenium. Chemosphere 264, 128417 ([CrossRef]).

Wang, L. Yuan, Deng, H., Zhang, Z., 2021b. Structural characterization and stability study of green synthesized starch stabilized silver nanoparticles loaded with isoorientin. Food Chem. 338, 127807–127809.

Xiang, L., Zhao, H.M., Li, Y.W., Huang, X.P., Wu, X.L., Zhai, T., Mo, C.H., 2015. Effects of the size and morphology of zinc oxide nanoparticles on the germination of Chinese cabbage seeds. Environ. Sci. Pollut. Control Ser. 22 (14), 10452–10462.

Zafar, H., Ali, A., Ali, J.S., Haq, I.U., Zia, M., 2016. Effect of ZnO nanoparticles on *Brassica nigra* seedlings and stem explants: growth dynamics and anti-oxidative response. Front. Plant Sci. 7, 535.

Zheng, Y.L., Hou, L.J., Liu, M., Newell, S.E., Yin, G.Y., Yu, C.D., Zhang, H.L., Li, X.F., Gao, D.Z., Gao, J., 2017. Effects of silver nanoparticles on nitrification and associated nitrous oxide production in aquatic environments. Sci. Adv. 3, 11 ([CrossRef]).